Ginzburg-Landau theory of oil-water-surfactant mixtures

G. Gompper and S. Zschocke
Sektion Physik der Ludwig-Maximilians-Universität München, 8000 München 2, Germany
(Received 9 June 1992)

A simple Ginzburg-Landau free-energy functional for oil-water-surfactant mixtures, with a single, scalar order parameter, is studied in detail. We show that the free energy of swollen spherical and cylindrical micelles obtained from this model can be described in terms of the Helfrich Hamiltonian of surfactant monolayers. The surface tension σ, the spontaneous curvature modulus λ, the saddle-splay modulus $\bar{\kappa}$, and the bending rigidity κ of the surfactant sheet at the oil-water interface can all be calculated from the order-parameter profile of the planar oil-water interface. It is demonstrated that for stable droplets and cylinders, these expressions of κ and $\bar{\kappa}$ give reliable predictions for the free energy only if the system is at oil-water coexistence. Off coexistence, the distortion of the profile due to the finite curvature of the interface has to be taken into account. The results are used to discuss the phase diagram of the Landau model. In addition to the bending elasticity, the interaction between monolayers plays an important role. This interaction is found to be always attractive in our model. We show that the simple Ginzburg-Landau theory describes various spatially modulated phases: the lamellar phase, the hexagonal phase of cylinders, a cubic crystal of spherical micelles, and bicontinuous cubic phases. Finally, we discuss the behavior of oil-water-surfactant mixtures near a wall. We find that under suitable conditions the lamellar phase wets the wall-oil (or wall-water) interface.

PACS number(s): 61.20.Gy, 82.65.Dp, 64.60.Cn

I. INTRODUCTION

The investigation of the properties of oil-water-surfactant mixtures has a long history. This is mainly due to their important applications in everyday life. On a microscopic scale, the most intriguing property of these systems is the self-assembly of the surfactant molecules into a large variety of complicated structures [1–3]. These can be visualized either as surfactant monolayers between oil-rich and water-rich regions, or as surfactant bilayers with oil or water on both sides, which fill the three-dimensional space in various ways. The lamellar phase, for example, is a simple, one-dimensional stacking of surfactant sheets, while the microemulsion is an (almost) random array of monolayers. There has been much interest in these systems recently, because an understanding of the statistical mechanics of self-avoiding surfaces [4,5] is also important in other areas of science, as for the behavior of cell membranes in biology [4–6], and for the string theory in high-energy physics [7].

Both experiments and theories of oil-water-surfactant systems have made considerable progress over the last years. On the theoretical side, much work has been investigated in the study of various lattice models [2,8–12]. The main advantage of these models is that many methods of statistical mechanics are available for lattice models. Their drawback is that oil-water-surfactant mixtures are in the continuum, so that the density distribution of many ordered phases seen in lattice models can only be a rough approximation of the real structures. It has been shown [8,11,12] that many results obtained for lattice models in the mean-field approximation change very little when the effect of fluctuations is included. However, on the level of finding configurations of minimal free energy, continuum models are conceptually not more difficult than lattice models, although the numerical effort to find the density profiles may be considerably larger. We investigate in this paper a simple continuum Landau-Ginzburg model for a single, scalar order parameter. This model has been introduced in Ref. [13] to explain the wetting behavior of oil-water interfaces by the microemulsion. We find that the phase diagram contains many of the ordered phases observed in experiment, and that the density profiles are much more realistic than anything found in lattice models. This includes, in particular, cubic phases with bicontinuous structure.

A complementary theoretical approach to oil-water-surfactant mixtures is phenomenological (or interfacial) models of microemulsions [2,14–19]. In this case, it is assumed that there is always a complete, incompressible monolayer at the microscopic oil-water interface. The monolayers are considered in this approach to be infinitely thin, mathematical surfaces. All the physics of the monolayers is subsumed in their elastic energy, which is given by the Helfrich Hamiltonian [14,20],

$$\mathcal{H}=\int dS\,[\sigma+\lambda H+2\kappa H^2+\bar{\kappa}K]\ , \tag{1}$$

where dS denotes the surface element. Here, $H=\frac{1}{2}(1/R_1+1/R_2)$ is the mean curvature and $K=1/R_1R_2$ the Gaussian curvature, both given in terms of the local principal radii of curvature R_1 and R_2. The first term in (1) is the surface tension σ. This term is often assumed to be negligibly small or to vanish altogether [21]. The second term gives the spontaneous curvature $H_0=-\lambda/(4\kappa)$. The elastic moduli κ and $\bar{\kappa}$ determine the bending rigidity of the monolayer. Expressions for the elastic bending moduli have been derived from

various microscopic models [22–26]. We have shown in Ref. [22] that the bending energy (1) can be derived from our Ginzburg-Landau model, under the assumption that the order-parameter profile of a curved interface can be approximated locally by the profile of a planar interface. We will give a more detailed derivation of this result in Sec. III below. The validity of this approximation can be determined by a systematic expansion of the order-parameter profile in the inverse radii of curvature. We will show that the lowest-order approximation for κ and $\bar{\kappa}$ gives reliable results only at oil-water *coexistence*. In Sec. IV, the effective interaction of planar oil-water interfaces is derived. The interaction is found to be always attractive, so that the transition from oil-water coexistence to the lamellar phase—or to other ordered phases—must be first order. In Sec. V we present phase diagrams of our model, and discuss the stability of the various phases in terms of the bending elasticity of the surfactant sheets. Section VI, finally, is devoted to the study of oil-water-surfactant mixtures near a wall. The wall favors planar interfaces, and can therefore induce complete wetting by the lamellar phase.

II. SIMPLE GINZBURG-LANDAU MODEL

Our analysis is based on the free-energy functional [13]

$$\mathcal{F}[\phi(\mathbf{r})]=\int d^3r\,[c(\nabla^2\phi)^2+g(\phi)(\nabla\phi)^2+f(\phi)-\mu\phi]\ , \tag{2}$$

for a scalar order-parameter field $\phi(\mathbf{r})$, which is proportional to the local difference of the oil and water concentrations. This functional does not contain explicitly the surfactant degrees of freedom, like the surfactant concentration. These degrees of freedom are considered as being integrated out [27,28]. The presence of the amphiphiles manifests itself in the special form [30,31] of the functions f and g. Three-phase coexistence of an oil-rich phase with $\phi=\phi_o$, a water-rich phase with $\phi=\phi_w$, and a microemulsion phase with $\phi=\phi_m$, which are all homogeneous phases, implies that the free-energy density f must have three local minima. We define the chemical potential difference μ between oil and water such that $\mu=0$ at oil-water coexistence. Thus, $f(\phi_o)=f(\phi_w)$. The value of the microemulsion minimum $f(\phi_m)$ obviously depends on the amount of amphiphile present: $f(\phi_m)$ is low for high amphiphile concentration and high for small amphiphile concentrations. The general structure of g follows from scattering experiments in the three homogeneous phases, which show that there is a pronounced peak in the scattering intensity at nonzero wave vector $\mathbf{q}$ in the microemulsion, but only a peak at $q=0$ in the oil-rich and water-rich phases. In the Gaussian approximation, the scattering intensity of our model (2) is given by

$$S(q)\sim[cq^4+g(\phi_b)q^2+\tfrac{1}{2}f''(\phi_b)]^{-1}\ , \tag{3}$$

where $\phi_b\in\{\phi_o,\phi_m,\phi_w\}$. A peak at $q>0$ ($q=0$) is therefore equivalent with $g(\phi_b)<0$ [$g(\phi_b)>0$], as first noted by Teubner and Strey [32]. Thus, in an expansion of f and g in powers of the order parameter, we must have

$$\begin{aligned} f(\phi)&=\sum_{n=2}^{6}a_n\phi^n\ ,\\ g(\phi)&=\sum_{n=0}^{2}g_n\phi^n\ . \end{aligned} \tag{4}$$

Here, $a_6>0$ and $g_2>0$ is required for thermodynamic stability. The other coefficients $a_2,\ldots,a_5$ are chosen in such a way as to produce a function $f(\phi)$ with three minima, as discussed above. In the case of oil-water symmetry, the coefficients of the odd powers of ϕ in (4) all vanish identically. For numerical and analytical calculations, it is often convenient to use a piecewise parabolic form [33],

$$f(\phi)=\begin{cases}\omega_w(\phi-\phi_w)^2 & \text{for } \phi_{0+}<\phi\\ \omega_m\phi^2+f_0 & \text{for } \phi_{0-}<\phi<\phi_{0+}\\ \omega_o(\phi-\phi_o)^2 & \text{for } \phi<\phi_{0-}\ ,\end{cases} \tag{5a}$$

where ϕ_{0+} and ϕ_{0-} are defined such that f is continuous, and a piecewise constant form of g,

$$g(\phi)=\begin{cases}g_w & \text{for } \phi_{0+}<\phi\\ g_m & \text{for } \phi_{0-}<\phi<\phi_{0+}\\ g_o & \text{for } \phi<\phi_{0-}\ .\end{cases} \tag{5b}$$

In the case of oil-water symmetry, the matching points are $\phi_{0+}=-\phi_{0-}\equiv\phi_0$.

The order-parameter profile, which minimizes the free-energy functional (2), is determined by the Euler-Lagrange (EL) equation,

$$2c\Delta^2\phi-2g(\phi)\Delta\phi-g'(\phi)(\nabla\phi)^2+f'(\phi)-\mu=0\ , \tag{6}$$

where $g'=dg/d\phi$ and $f'=df/d\phi$.

III. ELASTIC PROPERTIES OF OIL-WATER INTERFACES: SWOLLEN MICELLES

Consider a large drop of oil with radius R, embedded in bulk water, with no amphiphile present. The total free energy of the system is a sum of bulk and interface contributions. The bulk term is the difference in bulk free energies of the two phases, the interface term is $\sigma[R]4\pi R^2$, the interfacial tension integrated over the whole interface. Here, the interface tension depends on the choice of the dividing surface, which is indicated by the argument in square brackets. The interface tension acts to minimize the interfacial area of the drop. Therefore, a stable drop is only possible if the interior phase (the oil phase) has a lower bulk free energy than the exterior phase (the water phase). The pressure difference p, between inside and outside, and the radius of the drop are related by the Laplace equation [34,35]

$$p=\frac{2\sigma[R]}{R}\ . \tag{7}$$

This implies that a stable drop is *not* possible at two-phase coexistence, where $p=0$, as long as $\sigma>0$. In a square-gradient Ginzburg-Landau theory [36] this can be seen easily by considering the Euler-Lagrange equation in

spherical coordinates,

$$\frac{d^2}{dr^2}\phi+\frac{2}{r}\frac{d}{dr}\phi=f'(\phi)-\mu\ , \tag{8}$$

where f is normalized in such a way that the free-energy density of the exterior phase vanishes. This equation corresponds to a mechanical particle moving in the potential $-[f(\phi)-\mu\phi]$, with a local friction coefficient $2/r$. Therefore, in order to reach the local maximum of the potential for $r\to\infty$, the particle has to start at $r=0$ with larger potential energy. Thus, the bulk free energy of the interior phase is lower than that of the exterior phase, in agreement with the previous considerations.

When amphiphile is added to the system, the situation changes. The amphiphiles have two effects. First, they reduce the interfacial tension, by forming a monolayer at the oil-water interface. Second, the monolayer has a preferred (spontaneous) radius of curvature and a bending rigidity, which, like the pressure p, can counteract the interfacial tension. If the interfacial tension is small enough, oil droplets in water become stable *at coexistence*. An analysis of the EL equation (6) of our Landau model (2) and (5) shows that indeed stable solutions appear for $p=0$ when the interfacial tension is small. It will become clear in Sec. V below how the parameters have to be chosen in order to obtain these solutions.

The interfacial free energy (per unit area) of a planar oil-water interface, located at $z=0$, is given by

$$\frac{F}{A}=\int_{-\infty}^{\infty}dz\left[c\left[\frac{\partial^2}{\partial z^2}\bar\phi(z)\right]^2+g(\bar\phi)\left[\frac{\partial}{\partial z}\bar\phi(z)\right]^2+f(\bar\phi)\right]\ . \tag{9}$$

Here, the profile $\bar\phi(z)$ satisfies the Euler-Lagrange equation (6). We have normalized f in such a way that $f(\phi_o)=f(\phi_w)=0$, where ϕ_o and ϕ_w are the values of the order parameter far away from the interface. In the planar case, the first integral of this equation is known to be [13]

$$2c\,[\bar\phi'\bar\phi'''-\tfrac{1}{2}(\bar\phi'')^2]-g(\bar\phi)(\bar\phi')^2+f(\bar\phi)=\text{const}\ , \tag{10}$$

where the constant vanishes identically for our normalization of f. For a cylinder and a sphere, both of radius R, one has similarly

$$\frac{F}{A}=\frac{1}{R^{d-1}}\int_0^{\infty}dr\,r^{d-1}\left[c\left[\frac{\partial^2}{\partial r^2}\phi_R(r)+\frac{d-1}{r}\frac{\partial}{\partial r}\phi_R(r)\right]^2+g(\phi_R)\left[\frac{\partial}{\partial r}\phi_R(r)\right]^2+f(\phi_R)-\mu\phi_R\right]\ , \tag{11}$$

where $d=2$ (3) for the cylinder (sphere). Here, ϕ_R is the profile which satisfies the EL equation (6) in cylindrical and spherical coordinates, respectively. Now, for large radii R, the profile $\phi_R(r)$ will approach the planar profile $\bar\phi(r-R)$. Therefore, we can try an expansion of the form [22,36]

$$\phi_R(r)=\bar\phi(r-R)+\frac{\phi_1(r-R)}{R}+\frac{\phi_2(r-R)}{R^2}+\cdots\ ,\qquad \mu=\frac{\mu_1}{R}+\frac{\mu_2}{R^2}+\cdots\ . \tag{12}$$

Let us first consider only the leading term in this expansion. When the planar profile is inserted for ϕ_R in Eq. (11), the invariant (10) can be used to eliminate f:

$$\int_0^{\infty}dr\,r^{d-1}f(\bar\phi)=\int_0^{\infty}dr\,r^{d-1}[g(\bar\phi)(\bar\phi')^2+3c(\bar\phi'')^2]-\delta_{d,3}2c\int_0^{\infty}dr(\bar\phi')^2\ . \tag{13}$$

After substituting $r\to r+R$, we obtain

$$\frac{F}{A}=\int_{-R}^{\infty}dr\left[1+\frac{r}{R}\right]^{d-1}\left[c\left[\bar\phi''+\frac{d-1}{R+r}\bar\phi'\right]^2+3c\bar\phi''^2+2g\bar\phi^2\right]-R^{-2}\delta_{d,3}2c\int_{-R}^{\infty}dr(\bar\phi')^2\ . \tag{14}$$

We expand in powers of R^{-1}, and extend the lower boundary of integration to $-\infty$, anticipating errors which are exponentially small in R. Then, the free energy of droplets and cylinders is given by

$$F_{\text{sphere}}=\sigma R^2+\lambda R+2\kappa+\bar\kappa\ ,\qquad F_{\text{cyl}}/L=\sigma R+\frac{\lambda}{2}R+\frac{\kappa}{2}+O(R^{-1})\ , \tag{15}$$

which is just the form of the Helfrich Hamiltonian, with

$$\sigma=\int_{-\infty}^{+\infty}dz\,p_s(z)\ , \tag{16a}$$

$$\lambda=2\int_{-\infty}^{+\infty}dz\,zp_s(z)\ , \tag{16b}$$

$$\kappa=\int_{-\infty}^{+\infty}dz[2c(\bar\phi')^2]\ , \tag{16c}$$

$$\bar\kappa+2\kappa=\int_{-\infty}^{+\infty}dz\,z^2p_s(z)\ , \tag{16d}$$

where

$$p_s(z)=[2g(\bar\phi)(\bar\phi')^2+4c(\bar\phi'')^2]\ . \tag{16e}$$

We have already shown in Ref. [22] that for the piecewise parabolic model (5), the free energy of a drop or cylinder as a function of the radius R, calculated from the Helfrich expression (1) with the elastic constants (16), agrees very well with the full free energy (11). Some details about the calculation of order-parameter profiles in the parabolic model will be presented in Sec. IV below. Here, we want to demonstrate that the equilibrium radius of drops and cylinders, as a function of the chemical potential of the amphiphile f_0, also agrees very well. In the case of the Helfrich Hamiltonian, the radius is easily calculated by minimizing (15), which implies

$$\bar R_{\text{sphere}}=-\frac{\lambda}{2\sigma},\quad \bar R_{\text{cyl}}=\left[\frac{\kappa}{2\sigma}\right]^{1/2}\ . \tag{17}$$

The f_0 dependence of the free energy per unit area is shown in Fig. 1(a), and the equilibrium radii of droplets and cylinders in Fig. 1(b). The agreement in both cases is excellent.

Several comments are in order. First, note that our result (16) agrees with the results obtained for the standard square-gradient theories, i.e., for $c=0$, $g=\text{const}>0$, in a low-temperature expansion [37–39]. In this case, $\kappa\equiv 0$ and $\bar{\kappa}>0$. Second, Helfrich [40] has given a purely mechanical derivation of the elastic moduli, which leads to the identification of $p_s(z)$ as the stress profile through the monolayer. However, the mechanical derivation gives a result for $\bar{\kappa}$, which agrees with (16d) only for $\kappa=0$, and makes no prediction for κ. We believe that this discrepancy is due to a change of the stress profile as the monolayer is bent, which is not taken into account in Ref. [40]. A typical stress profile of a monolayer, calculated from Eq. (16e), is shown in Fig. 2. Third, the freedom in the choice of the dividing surface (which defines the position of the interface for a given order-parameter profile) has been discussed in Ref. [22], a discussion we do not want to repeat here. However, it is important to note that the results [(16a) and (16c)] for the interfacial tension σ and the bending rigidity κ are *independent* of this choice. In this paper, we always use the equimolar surface to define the position of the interface.

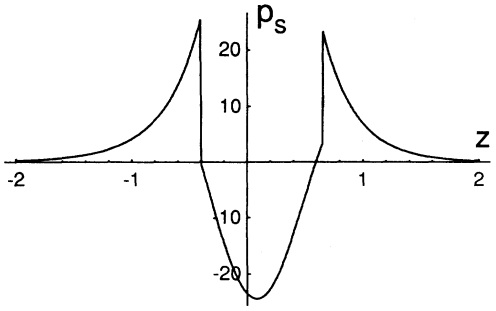

FIG. 2. Stress profile $p_s(z)$ through the monolayer, Eq. (16e), for the piecewise parabolic model (5). The parameters are the same as in Fig. 1, and $f_0=1.42$.

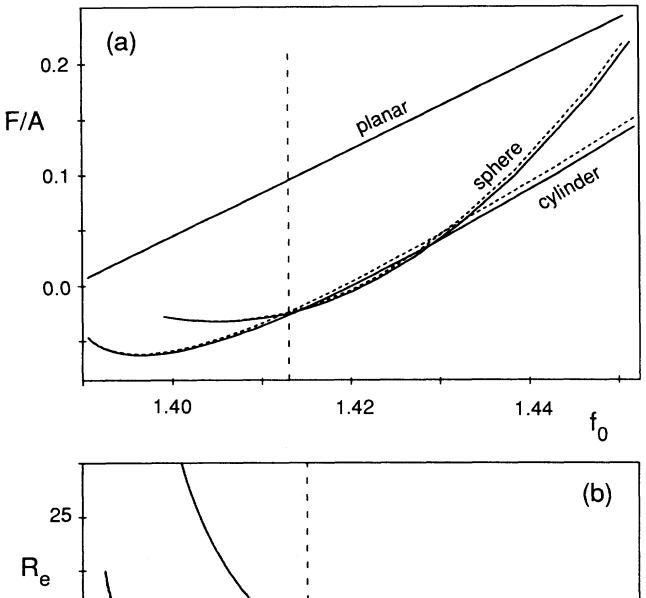

FIG. 1. (a) Free energy per unit area of stable droplets, cylinders, and planar oil-water interfaces and (b) equilibrium radius of droplets and cylinders, both as a function of the parameter f_0 (related to the surfactant chemical potential) of the piecewise parabolic model (5), with $c=1$, $g_w=g_o=4.6$, $g_m=-4.5$, $\omega_w=\omega_o=4$, $\omega_m=1$, $\phi_w=2$, and $\phi_o=-1$. The full lines are obtained from the full EL equation; the dotted lines are calculated from the Helfrich expression (1) with the elastic moduli (16). The vertical dashed line marks the transition to a spatially modulated phase (see Sec. V).

For the case of droplets and cylinders stabilized by a pressure difference, i.e., off oil-water coexistence, we want to calculate now the corrections to the free energy, which arise from the fact that for a drop or cylinder of finite radius the order parameter profile deviates from the planar profile. We assume that the order-parameter profile as well as the chemical potential difference between inside and outside can be expanded in a power series in the inverse radius R^{-1} of droplets and cylinders around the planar profile (with $R^{-1}=0$), see Eq. (12). This calculation is somewhat tedious, and is therefore delegated to Appendix B. The result of this calculation is, see Eq. (B30),

$$F[\phi]=F_b[\phi]+F_s[\bar{\phi}] - AR^{-2}\int_{-\infty}^{\infty} dr\{(d-1)[g(\bar{\phi})\bar{\phi}'\phi_1+2c\bar{\phi}''\phi_1']+\tfrac{1}{2}\mu_1 r\phi_1'\}\ , \tag{18}$$

where A is the area of the interface, and [see Eq. (B7)]

$$\int dr\,\mu_1\bar{\phi}'=-(d-1)\sigma_\infty\ . \tag{19}$$

With (12), $\mu=\mu_1/R+\cdots$, (19) can be easily recognized as the Laplace equation (7).

For the square-gradient theories with piecewise parabolic free-energy density f, the free energy of spheres and cylinders can be calculated exactly. This gives us the opportunity to check the result (18) explicitly. It is shown in Appendix C that the two expressions do indeed agree to order R^{-2}.

Thus, the distortion of the profile gives correction terms to the interfacial free energy F_s/A of the order R^{-2}, terms which can be comparable in size with the contributions (16) of κ and $\bar{\kappa}$. These correction terms depend via ϕ_1 on the geometry of the interface in a rather

complicated way. Since we have studied only two geometries of the interface, our result can always be expressed in terms of renormalized values of κ and $\bar{\kappa}$. In order to check the validity of the Helfrich Hamiltonian, we would need to consider at least a third geometry. The results of Appendix C imply that for droplets *off* oil-water coexistence, the correction term in (18) can be much larger than the approximation (16d) for $\bar{\kappa}$, so that the expression (16d) is of little use in this case.

IV. TRANSITION TO THE LAMELLAR PHASE: EFFECTIVE INTERACTIONS BETWEEN MONOLAYERS

In addition to the three homogeneous phases, oil, water, and microemulsion, our Landau models contain various spatially modulated phases, in particular the lamellar phase. This can be most easily seen from the behavior of the scattering intensity (3). For large, negative g_m (this can be achieved by increasing the surfactant concentration, or their amphiphilicity), the scattering intensity in the microemulsion develops a singularity at a finite wave vector q^*. This signals the existence of a transition to a modulated phase, with a typical length scale of order $2\pi/q^*$.

The transition from the homogeneous ordered phases, oil and water, to the lamellar phase is driven by two physical mechanisms: (i) the reduction of the interfacial tension of the oil-water interface, and (ii) the interaction between these interfaces. Both effects can be studied by considering *two* oil-water interfaces, located at a distance $2l$ apart, and calculating the free energy as a function of the distance $2l$. For very large separation of the two interfaces, the profile becomes a simple superposition of two oil-water interfacial profiles, and the free energy is twice the interfacial tension of the oil-water interface. For smaller separations $2l$, the free energy has also a contribution from the interaction of the two interfaces, which we want to extract [41–44]. We consider again the piecewise parabolic model. However, the same methods can be used for more general forms of f and g as well.

For the piecewise parabolic model, the general solution of the EL equations for an order-parameter profile, varying in one dimension z, within one parabola $i \in \{o,w,m\}$, i.e., the parabola describing the oil, water, or microemulsion phase, respectively, is given by

$$\phi_i(z)=\sum_{j=1}^{4} C_{ij} e^{\gamma_{ij} z} , \tag{20}$$

where the exponents γ_{ij} are solutions of the characteristic equation

$$c\gamma_{ij}^4 - g_i \gamma_{ij}^2 + \omega_i = 0 . \tag{21}$$

For $g_i > \sqrt{4c\omega_i} \equiv g_{\mathrm{do},i}$, all solutions γ_{ij} of (21) are real, whereas for $g_i < g_{\mathrm{do},i}$ all solutions are complex (and differ only in the sign of their real and complex parts). In the bulk microemulsion phase, $g_m = g_{\mathrm{do},m}$ is called the disorder line [45]. Its significance is that the bulk correlation function changes from simple exponential decay to an exponentially damped oscillation at this line, and thus distinguishes ordinary and structured fluids [11].

The full profile is obtained by matching the partial solutions in the various parabola. The amplitudes are then determined from the condition that the profile and its first and second derivatives, plus the invariant (10), be continuous everywhere. For the symmetric oil-water profile, one has

$$\phi(z)=\begin{cases} \bar{B}_1 \sinh(\beta_1 z)+\bar{B}_2 \sinh(\beta_2 z), & z\in[0,l_1] \\ \phi_w + \bar{A}_1 e^{-\alpha_1 z}+\bar{A}_2 e^{-\alpha_2 z}, & z > l_1 \end{cases} \tag{22}$$

and $\phi(-z)=-\phi(z)$. We will frequently denote the oil-water profile as the "kink" below. The exponents $\alpha_{1,2}$ and $\beta_{1,2}$ denote the solutions with positive real parts of the characteristic equations (21) in the outer and inner parabola, respectively. The amplitudes $\bar{A}_1$, $\bar{A}_2$, $\bar{B}_1$, and $\bar{B}_2$ and the length scale l_1 are determined by the continuity conditions at $z=l_1$. This can only be done numerically.

For the double-kink profile of an oil-layer in water, we make the ansatz

$$\phi(z)=\begin{cases} -\phi_w + A_1 \cosh(\alpha_1 z)+A_2 \cosh(\alpha_2 z), & z\in[0,l-l_1] \\ \sum_{i=1}^{4} B_i e^{\beta_i (z-l)}, & z\in[l-l_1,l+l_1] \\ +\phi_\omega + C_1 e^{-\alpha_1(z-l-l_1)}+C_2 e^{-\alpha_2(z-l-l_1)}, & z\in[l+l_1,\infty] \end{cases} \tag{23}$$

and $\phi(-z)=\phi(z)$. Here, $2l_1$ is the "width" of a single oil-water interface. The eight amplitudes $A_1, A_2, B_i, i=1,\ldots,4$ and C_1, C_2 and the two length scales l and l_1 are determined by the continuity conditions at $z=l-l_1\equiv l_0$ and $z=l+l_1$, as discussed above. Here, we want to minimize F with the additional constraint that the distance of the two interfaces is $2l$. We therefore have to give up one of these matching conditions, the continuity of the invariant (10). In order to get an analytic result, we assume that compared to an infinite separation of the two kinks, only the central part of the profile, in the interval $[-l_0,+l_0]$, is modified. In this case, only the continuity of the profile and the first derivative at $z=\pm l_0$ can be maintained. This leads to the amplitudes

$$A_{1,2}\cosh(\alpha_{1,2} l_0)=\frac{\phi_0' - \tilde{\phi}_0 \alpha_{2,1} \tanh(\alpha_{2,1} l_0)}{\alpha_{1,2}\tanh(\alpha_{1,2} l_0)-\alpha_{2,1}\tanh(\alpha_{2,1} l_0)} . \tag{24}$$

Here, $\tilde{\phi}_0=\phi_w-\phi_0$ and ϕ_0' is the derivative of the kink profile at $\phi=\phi_0\equiv\phi_{0+}$, determined numerically. The profile (23) with the amplitudes (24) can then be inserted into (2) to calculate the free energy. The result is a lengthy expression which we do not want to reproduce here. It can be expanded for large $l=l_0+l_1$, which yields the asymptotic behavior

$$F[2l]=2F_{\text{kink}}+V_1 e^{-2\alpha_1 l_0}+V_2 e^{-2\alpha_2 l_0}+\cdots \quad (25)$$

with $\mathrm{Re}(\alpha_1)<\mathrm{Re}(\alpha_2)$, where

$$V_{1,2}=\pm\frac{4c(\alpha_1+\alpha_2)\alpha_{1,2}(\alpha_{2,1}\tilde{\phi}_0-\phi_0')^2}{\alpha_1-\alpha_2} . \quad (26)$$

For $g_w > g_{\text{do},w}$, where $g_{\text{do},w}$ is the disorder line of the water-rich phase, the amplitude of the contribution with the slowest decay in (25) V_1 is always negative, so that the effective interaction is always attractive at large distances. Since $V_2>0$, there is a global minimum at a finite distance of the two kinks. For $g_w < g_{\text{do},w}$, the effective interaction oscillates, with the first minimum of the interaction potential being the global minimum. Thus, in both cases there is an attractive interaction between oil-water interfaces, so that the transition from oil-water coexistence to a lamellar phase is always first order (this may change when fluctuation effects are taken into account). The transition occurs when the positive interfacial tension is just balanced by the attractive interaction. We can conclude that the transition from oil-water coexistence to the lamellar phase is driven by the decrease of the oil-water interfacial tension.

However, there are two possible exceptions: (i) when $(\alpha_1\tilde{\phi}_0-\phi_0')\to 0$, so that $V_1\to 0^-$, and (ii) for $g_w\to g_{\text{do},w}$, so that $(\alpha_1-\alpha_2)\to 0$. For the equilibrium distance $\bar{l}_0$ we obtain from (25) and (26)

$$2(\alpha_1-\alpha_2)\bar{l}_0=\ln\left[\frac{\alpha_1^2(\alpha_2\tilde{\phi}_0-\phi_0')^2}{\alpha_2^2(\alpha_1\tilde{\phi}_0-\phi_0')^2}\right] . \quad (27)$$

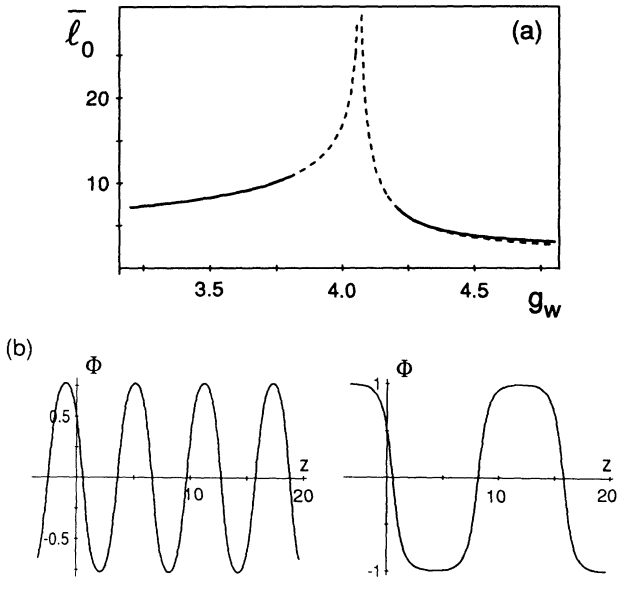

FIG. 3. System with oil-water symmetry. (a) The equilibrium thickness $\bar{l}_0$ of an oil layer in water, as a function of g_w, along the line $\sigma=0$; the dashed line is the approximation (27), the full line is the solution of the EL equations. (b) Order-parameter profiles of the lamellar phase at coexistence with oil and water, for $g_w=4.8$ and 4.19. The calculations are for the piecewise parabolic model (5) with the parameters $c=1$, $g_m=-4.5$, $\omega_w=\omega_o=4$, $\omega_m=1$, $\phi_w=1$, and $\phi_o=-1$.

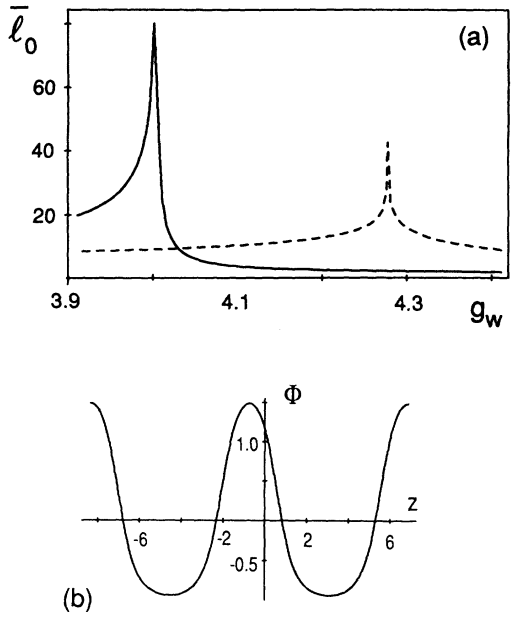

FIG. 4. System with broken oil-water symmetry. (a) The equilibrium thickness $\bar{l}_0$ of an oil layer in water (dashed line), and of a water layer in oil (full line), as a function of $g_w=g_o$, along the line $\sigma=0$. Both curves are calculated from Eq. (27). (b) Order-parameter profile of the lamellar phase at coexistence with oil and water, for $g_w=4.6$ and $f_0=1.413$. The calculations are for the piecewise parabolic model (5) with the parameters $c=1$, $g_m=-4.5$, $\omega_w=\omega_o=4$, $\omega_m=1$, $\phi_w=2$, and $\phi_o=-1$.

The limit $g_w\to g_{\text{do},w}$ can be made in (27) and leads to a *finite* separation $\bar{l}_0$ at the disorder line of the water-rich phase. The numerical analysis of Eqs. (25) and (26) shows, however, that V_1 vanishes at a point g^* in the vicinity of the disorder line. The kink separation is expected to diverge logarithmically at this point. Our numerical and analytical results for the equilibrium distance of two kinks are shown in Fig. 3(a). The approximation (25) and (26) is obviously very good.

We have calculated the interaction of two interfaces in order to predict the spacing of monolayers in the lamellar phase. Indeed, the lattice spacing of the lamellar phase shows the swelling behavior as $g_w\to g^*$, as demonstrated in Fig. 3(b). Thus, for the special case $g_w=g^*$, the phase transition from oil-water coexistence to the lamellar phase should be a second-order transition.

The interaction of oil-water interfaces can also be calculated in the case of broken oil-water symmetry. We use again the piecewise parabolic model, with $g_w=g_o$. In this case, the thickness of an oil layer in water diverges at a different value of g_w than the thickness of a water layer in oil. This is shown in Fig. 4(a). The asymmetric order-parameter profile of the lamellar phase can be seen in Fig. 4(b). Thus, in the case of broken oil-water symmetry, the lamellar phase can be swollen by either increasing its water or its oil content.

V. PHASE DIAGRAMS

Our Landau model has three homogeneous phases by construction. We have already argued in the preceding section that there is also a lamellar phase at large, negative g_m. In fact, there are other spatially modulated phases, which we want to present now, together with the location of the phase transitions between them. There are some technical reasons, which will become clear below, to present results for both the piecewise parabolic model and the ϕ^6 model.

A. Piecewise parabolic model

The advantage of the piecewise parabolic model is that all order-parameter profiles, which vary in a single coordinate, can be calculated very easily with very high numerical precision. In particular, the expressions (16) for the elastic moduli of the oil-water interface can be evaluated almost exactly. However, this advantage turns into a disadvantage for the calculation of order-parameter profiles, which vary in several coordinates, because the loci of the matching points become one- or two-dimensional hypersurfaces, which themselves have to be determined numerically.

We have used two approaches to determine the order-parameter profiles and free energies of modulated phases in two and three coordinates. The first is the *effective interaction approach,* which works for hexagonal crystals of cylindrical, and for cubic crystals of spherical micelles. The idea is that we can use the results (25) and (26) for the effective interaction of planar interfaces also for (weakly) curved interfaces. Consider two spheres of radius R, with their centers located at $z=\pm D/2$. We assume that the total interaction energy can be obtained by integrating the effective interaction $V_{\rm eff}(d)$ over the projection of the spheres into the $z=0$ plane. Here $d=[D-2(R^2-x^2)^{1/2}]$ is the distance of two pieces of the micellar surface in the z direction, with distance x from the axis of rotational symmetry (the z axis). Thus, the total interaction energy is given in this approximation by

$$V_s(D,R)=\int_0^R dx\, 2\pi x V_{\rm eff}[D-2(R^2-x^2)^{1/2}] = \sum_{i=1}^{2} \frac{\pi V_i R}{\alpha_i} e^{-\alpha_i(D-2R)} \times \left[1-\frac{1}{2\alpha_i R}(1-e^{-2\alpha_i R})\right] . \quad (28)$$

A similar expression can be obtained for cylinders. This approach works best when the packing of spheres or cylinders is rather loose, so that the form of the interaction used in (28) is a good approximation. The second is the *Fourier approach,* where the order parameter is written as a Fourier series,

$$\phi(\mathbf{r})=\sum_{i=0}^{N}\sum_{\mathbf{K}\in B_i}\phi_{\mathbf{K}}\cos(\mathbf{K}\cdot\mathbf{r}) . \quad (29)$$

The sum runs over all reciprocal lattice vectors of the studied lattice structure, where B_i denotes the ith shell of the reciprocal lattice (i.e., reciprocal lattice vectors which are all related by symmetry operations). Since all the lattices considered here have point symmetry, $\sin(\mathbf{K}\cdot\mathbf{r})$ terms in (29) are not required. In practice, the sum has to be restricted to a limited number of shells, of course. This approach works best (i.e., the series converges most rapidly) when the cylinders are at close distances, so that all length scales are of comparable size. As mentioned above, it requires a large computational effort, because the loci of the matching points have to be determined in each step of the minimization procedure. Therefore, we have used it only for the two-dimensional, hexagonal lattice. The Fourier approach (with finite N) yields an upper bound for the local minima of the free-energy functional.

The free energies of fcc crystal, hexagonal, and lamellar phases are shown in Fig. 5 as a function of f_0. Since the free energies of all phases fall on almost parallel lines, a small difference in slope, like for the free energy of the hexagonal phase from the effective interaction and the Fourier approaches, can make a relatively large difference in the position of the phase boundaries, or determine if a phase appears at all in the phase diagram. From diagrams like Fig. 5 for various values of g_m, we have constructed the phase diagrams shown in Fig. 6. Figure 6(a) is the phase diagram of a system with oil-water symmetry, while this symmetry is broken in the phase diagram of Fig. 6(b). In the latter case, the results for the hexagonal phase from the Fourier approach have been used. The order-parameter profile of the hexagonal phase is shown in Fig. 7.

Now, we want to compare these phase diagrams with the results for the elastic moduli, which are shown in Fig. 8 as a function of f_0 and g_m. The first point to note is that in both the symmetric and the asymmetric case, the general behavior of σ, κ, and $\bar{\kappa}$ is very similar. Also, in both cases the transition from oil-water coexistence to the spatially modulated phases occurs very close to the line

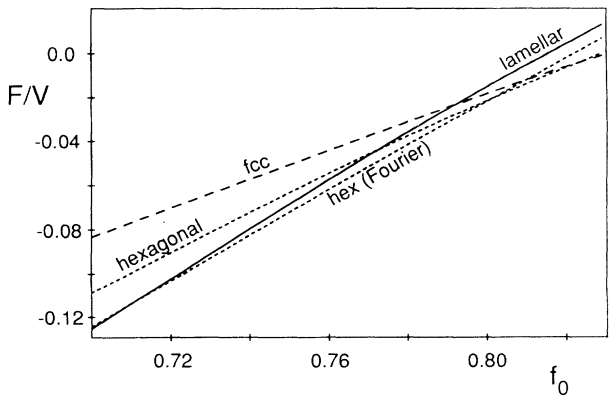

FIG. 5. Free energy densities of lamellar, hexagonal, and cubic phases, as a function of f_0, for the piecewise parabolic model with the parameters $c=1$, $g_o=g_w=4.6$, $g_m=-3.5$, $\omega_o=\omega_w=4$, $\omega_m=1$, $\phi_w=2$, and $\phi_o=-1$. The free energy of the cubic phase is calculated with the effective interaction approximation, the free energy of the hexagonal phase by both approximations, as discussed in the text.

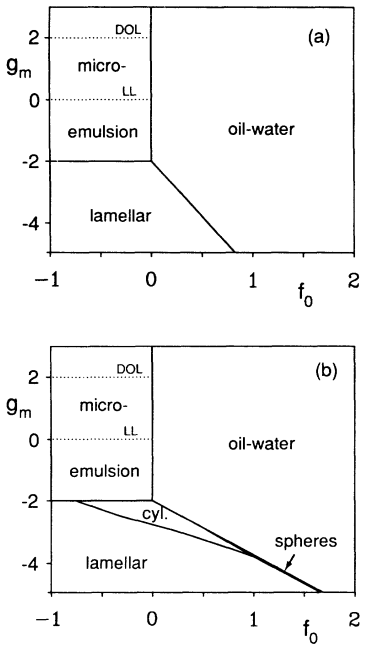

FIG. 6. Phase diagrams of the piecewise parabolic model. (a) System with oil-water symmetry ($\phi_w=1$, $\phi_o=-1$). (b) System with broken oil-water symmetry ($\phi_w=2$, $\phi_o=-1$). All other parameters are identical in both cases, $c=1$, $g_o=g_w=4.6$, $\omega_o=\omega_w=4$, and $\omega_m=1$. The correlation function changes its behavior at the disorder line (DOL) from oscillatory to monotonic. The peak of the scattering intensity moves away from wave vector $q=0$ at the Lifshitz line (LL).

where the interfacial tension of the oil-water interface vanishes. The deviation of the line of phase transitions from the line $\sigma=0$ is a measure for the magnitude of the attractive interaction between monolayers. In the *symmetric* case, Fig. 8(a), the spontaneous curvature vanishes identically. Therefore, we expect to see only modulated phases with zero mean curvature, the lamellar phase, or an ordered bicontinuous phase. This is indeed what is seen in Fig. 6(a). Due to the large computational effort required, we have not been able to study the stability of the bicontinuous phase here. This will be done in the next subsection. In the *asymmetric* case, Fig. 8(b), the spontaneous curvature is nonzero, and cubic phases of swollen micelles, as well as hexagonal phases of cylinders, can be expected, as are indeed found in the phase diagram, Fig. 6(b). The saddle-splay modulus is negative over a large part of the $\sigma=0$ line, which indicates the existence of droplet phase, again in agreement with the calculated phase diagram. These structures seem also to be favored below the $\sigma=0$ line by the negative saddle-splay modulus $\bar{\kappa}$; however, with increasing surfactant concen-

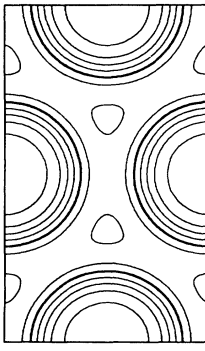

FIG. 7. Contour plot of the order-parameter distribution in the hexagonal phase for the piecewise parabolic model. The interior phase is water. The distribution is calculated by the Fourier approach with 12 shells. The parameters are the same as in Fig. 6(b), and $f_0=0.808$, $g_m=-3.5$.

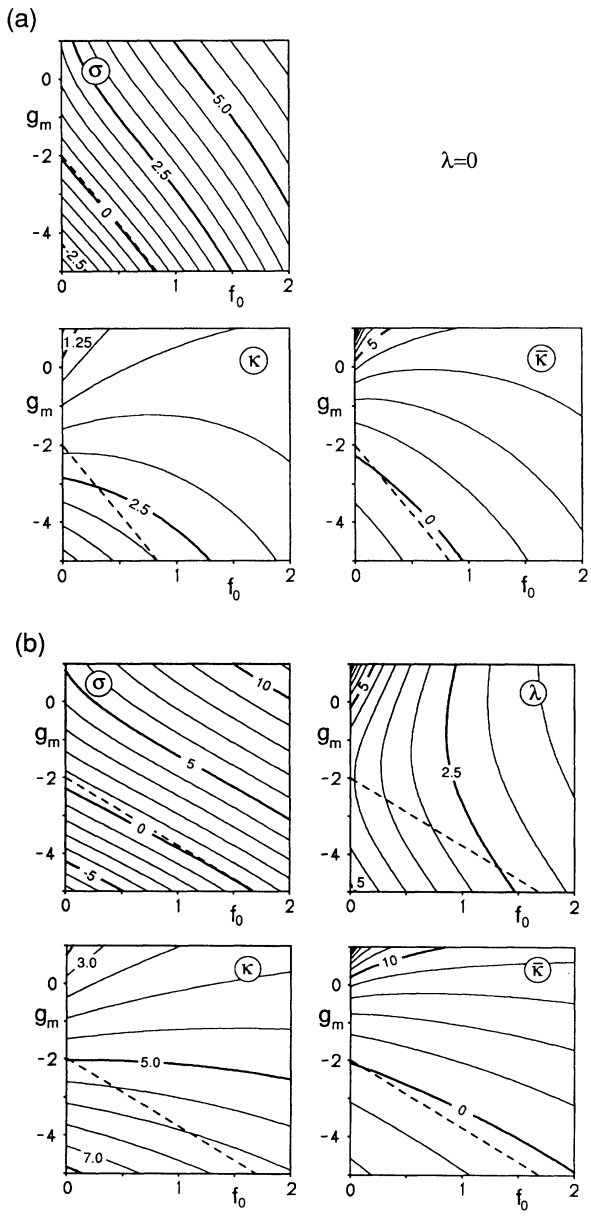

FIG. 8. Contour plots of the interface tension σ, the spontaneous curvature modulus λ, the saddle-splay modulus $\bar{\kappa}$, and the bending rigidity κ for (a) a system with oil-water symmetry, and (b) a system with broken oil-water symmetry. The parameters are the same as in Fig. 6. The dashed line marks the position of the phase transition between oil-water coexistence and the spatially modulated phases.

tration (which is favored by small or negative f_0 and large and negative g_m), the packing constraints always favor the lamellar phase. Finally, there is a small interval of positive $\bar{\kappa}$ along the $\sigma=0$ line, where bicontinuous structures can be expected. We will study in the next subsection if these structures can be stable in this region of the phase diagram.

B. ϕ^6 model

We now turn to the Landau free energy with $g(\phi)$ and $f(\phi)$ given by the polynomials (4). The purpose of this section is to investigate the stability of bicontinuous cubic phases in the phase diagram. We therefore restrict ourselves to the symmetric model, with $\phi\rightarrow-\phi$ symmetry. Here, the particular form for f,

$$f(\phi)=(\phi-\phi_b)^2(\phi+\phi_b)^2(\phi^2+f_0) \tag{30}$$

with $\phi_b=1$, is used (we also set $c=1$). We can get a very good estimate for the transition line from oil-water coexistence to the lamellar phase, by approximating the oil-water interfacial profile by [46]

$$\phi(z)=\phi_b\tanh(z/\xi) \tag{31}$$

and identifying the transition with the line where the interfacial tension vanishes. A minimization of the free-energy functional with respect to ξ yields

$$\xi^{-4}+\frac{5g_0+g_2}{12}\xi^{-2}-\frac{1+5f_0}{12}=0\ . \tag{32}$$

The condition that the surface tension vanishes gives another equation for ξ:

$$\xi^{-4}+\frac{5g_0+g_2}{4}\xi^{-2}+\frac{1+5f_0}{4}=0\ . \tag{33}$$

These two equations combined give the simple approximation

$$1+5f_0=\left[\frac{5g_0+g_2}{4}\right]^2 \tag{34}$$

for the location of oil-water-lamellar coexistence. We will see below that (34) is a remarkably good approximation for the transition line.

The phases we have compared are the lamellar phase, the simple-cubic (sc) bicontinuous phase, for which the $\phi(\mathbf{r})=0$ surface is the Schwarz P surface, and the single-diamond (sd) bicontinuous phase, for which the $\phi(\mathbf{r})=0$ surface is the Schwarz D surface [3]. The free energies of all these phases are calculated with the Fourier approach (29). For the sc phase, with lattice constant a, we have the symmetry

$$\phi\left[\mathbf{r}+\frac{a}{2}(1,1,1)\right]=-\phi(\mathbf{r}) \tag{35}$$

so that only the lattice vectors $\mathbf{K}=(2\pi/a)(n_1,n_2,n_3)$ with $(n_1+n_2+n_3)$ odd have nonvanishing amplitude. For the sd phase, a fcc lattice with basis $\mathbf{d}_\pm=\pm(a/4)(1,1,1)$, the symmetry relation (35) also holds, so that only Fourier components of lattice vectors with $\{n_1,n_2,n_3\}$ all odd contribute in this case.

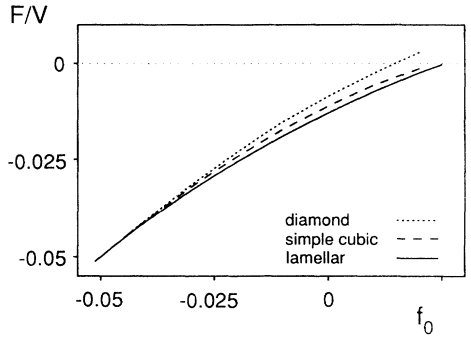

FIG. 9. Free-energy densities of lamellar, cubic bicontinuous, and diamond bicontinuous phases, as a function of f_0, for the ϕ^6 model [(4) and (30)] with the parameters $c=1$, $\phi_b=1$, $g_0=-2.1$, and $g_2=4\sqrt{1+f_0}-g_0+0.1$. The number of shells used in the Fourier series (29) was $N\leq 25$ for the simple-cubic phase, and $N\leq 12$ for the diamond phase.

The free energy of these three modulated phases is shown in Fig. 9 as a function of f_0, for $g_0=-2.1$, which is the region of the phase diagram where $\bar{\kappa}$ was found to be positive in Sec. V A. The lamellar phase is found to be the phase with the lowest free energy in the whole range from coexistence with the microemulsion to coexistence with oil and water. However, as the transition to the microemulsion is approached, the free energies of the bicontinuous phases and the lamellar phase become essentially degenerate. Although this means that the bicontinuous phases are not stable in the phase diagram (at least not for the parameter values investigated so far), this result indicates that the microemulsion itself should have a bicontinuous structure. The order-parameter distributions of the ordered bicontinuous phases are shown in Fig. 10.

Thus we arrive at the phase diagram of the ϕ^6 model shown in Fig. 11. As mentioned above, the approximation (34) for the lamellar $\rightarrow$ oil-water transition works so well that it is essentially indistinguishable in Fig. 11 from the true transition line. The transition from the lamellar phase to the microemulsion is second order, and is therefore located at $g_0=-g_{\mathrm{do},m}=-2\sqrt{1-2f_0}$. Note that in contrast to the piecewise parabolic model of the preceding subsection, the disorder line is here a function of f_0.

VI. WETTING OF A WALL BY THE LAMELLAR PHASE

When a first-order transition between two phases γ_1 and γ_2 is approached from the side of the γ_1 phase, the nucleation of γ_2 often occurs at the walls of the container, if the walls favor this phase [47,48]. Two situations can occur.

(i) The thickness of the layer of the γ_2 phase stays finite, when the γ_1/γ_2 coexistence is reached. This is called incomplete wetting.

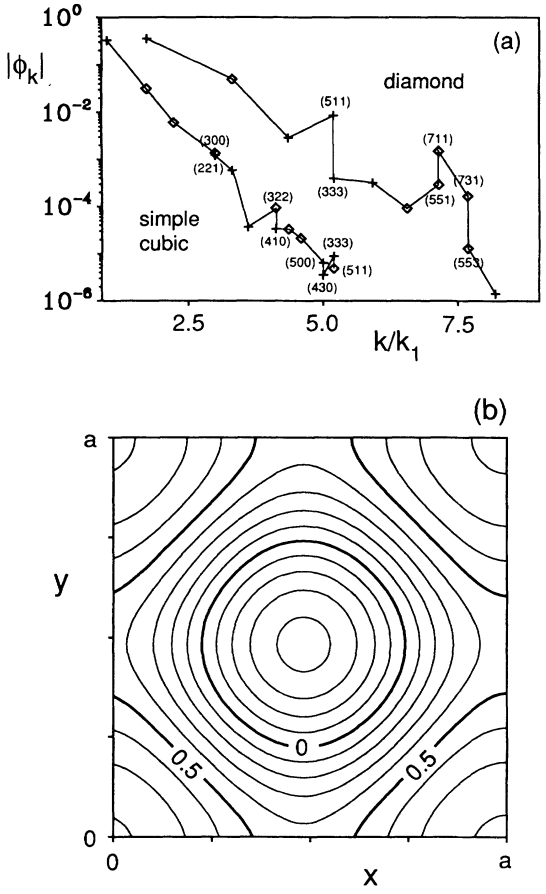

FIG. 10. Order-parameter distribution in the bicontinuous phases, for the ϕ^6 model [(4) and (30)] with $f_0=0.0001$; all other parameters are the same as in Fig. 9. (a) Fourier components of the simple cubic (lattice constant $a=7.78$) and the diamond phase ($a=17.64$). The crosses (+) indicate positive, the diamonds (◇) negative amplitudes. k_1 is the magnitude of the shortest wave vector. (b) Contour plot of the order parameter in the plane $z=0$ for the simple-cubic phase.

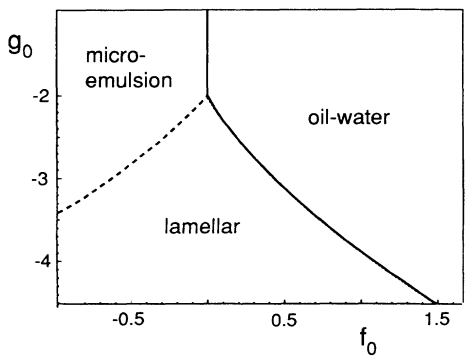

FIG. 11. Phase diagram for the ϕ^6 model [(4), and (30)] with $c=1$, $\phi_b=1$, and $g_2=4\sqrt{1+f_0}-g_0+0.1$. The dashed line indicates a second-order transition. The dotted line is the approximation (34) for the lamellar → oil-water transition; it is essentially indistinguishable from the true transition line.

(ii) The thickness of the γ_2 layer diverges at coexistence. This is called complete wetting.

We want to consider here a system, which is at oil-water coexistence, but the whole system is prepared in the oil phase (γ_1). When the chemical potential of the amphiphile increases, the system is driven towards the first-order transition to the lamellar phase (γ_2). Since the wall is a planar defect, we think it is reasonable to expect that the lamellar phase will be nucleated by the wall. We want to find out under what circumstances complete wetting occurs.

The wall can be attractive for either oil or water. This is described by a local chemical potential μ_s at the wall. Furthermore, the interactions of the molecules and their entropy (missing neighbors) will in general be different at the surface, as compared to the bulk. This is usually described in square-gradient theories by a local interaction term $f_s(\phi)=\omega_s\phi^2$. Since our Landau model involves additional derivatives in the bulk, we also want to include a gradient term $g_s(\phi)(\nabla\phi)^2$ at the surface. This term is related to a local chemical potential of the amphiphile at the wall. Here, we take $g_s(\phi)=g_s=\text{const}$. Thus, to study the behavior of oil-water-surfactant mixtures near a wall, we consider a free-energy functional of the form

$$\mathcal{F}[\phi]=\int_V d^dr\mathcal{L}_v[\phi,\nabla\phi,\nabla^2\phi]+\int_{\partial V}d^{d-1}r\mathcal{L}_s[\phi,\nabla\phi] \tag{36}$$

with

$$\mathcal{L}_s=f_s(\phi)+\mu_s\phi+g_s(\phi)(\nabla\phi)^2\ . \tag{37}$$

The Euler-Lagrange equations are obtained as usual from the first variation of $\mathcal{F}$:

$$\begin{aligned}\delta\mathcal{F}=&\int_V d^dr\left[\frac{\delta\mathcal{L}_v}{\delta\phi}-\nabla\frac{\delta\mathcal{L}_v}{\delta(\nabla\phi)}+\Delta\frac{\delta\mathcal{L}_v}{\delta(\Delta\phi)}\right]\delta\phi\\&+\int_{\partial V}d^{d-1}r\left[\frac{\delta\mathcal{L}_v}{\delta(\nabla\phi)}\mathbf{n}-\nabla\left[\frac{\delta\mathcal{L}_v}{\delta(\Delta\phi)}\right]\mathbf{n}+\frac{\delta\mathcal{L}_s}{\delta\phi}\right]\delta\phi\\&+\int_{\partial V}d^{d-1}r\left[\frac{\delta\mathcal{L}_v}{\delta(\Delta\phi)}\mathbf{n}+\frac{\delta\mathcal{L}_s}{\delta(\nabla\phi)}\right]\nabla(\delta\phi)\ ,\end{aligned} \tag{38}$$

where $\mathbf{n}$ is the surface normal, directed outward. To derive (38), Gauss's integral theorem has been used repeatedly. We see from (38) that in addition to the bulk EL equation, which follows for the fact that the first integral must vanish identically, there must be *two* boundary conditions, since the integrands of the last integrals must also vanish identically at any point of the boundary. With $\mathcal{L}_v=f(\phi)+g(\phi)(\nabla\phi)^2+c(\Delta\phi)^2$ and $\mathcal{L}_s$ from Eq. (37), the boundary conditions are

$$\begin{aligned}0&=2g(\phi)(\nabla\phi)\mathbf{n}-2c(\nabla\Delta\phi)\mathbf{n}+g_s'(\phi)(\nabla\phi)^2+f_s'(\phi)+\mu_s\ ,\\0&=c(\Delta\phi)\mathbf{n}+g_s(\phi)\nabla\phi\ .\end{aligned} \tag{39}$$

For the special case of planar walls, and $f_s(\phi)=\omega_s\phi^2$, $g_s(\phi)=g_s=\text{const}$, (39) reduces to

$$0=\pm 2g(\phi)\phi' \mp 2c\phi''' + 2\omega_s\phi + \mu_s \ ,$$
$$0=\pm c\phi'' + g_s\phi' \ , \tag{40}$$

where the upper (lower) sign applies to the right (left) wall. The EL equation is a fourth-order ordinary differential equation so that two boundary conditions on each side determine a discrete set of solutions.

The wetting behavior of the wall-oil interface by water is expected to be identical for our Landau model with the wetting behavior in the ϕ^4 model, where it has been studied extensively [47,48]. In our model, however, there is also the possibility of a wetting of the wall-oil interface by the lamellar phase, as the oil-water-lamellar coexistence is approached from the oil-water side. We want to study a semi-infinite system in the half space $z \geq 0$, so that there are two boundary conditions at $z=0$, plus the asymptotic convergence to the bulk oil phase for $z \to \infty$. For a system with oil-water symmetry, the order-parameter profile has the form

$$\phi(z)=\phi_i(z-l_i) \quad \text{for } z\in[l_i,l_{i+1}], \quad i\in\{0,1,\ldots,k\} \ ,$$
$$l_0=0<l_1<\cdots<l_{k+1}=\infty \ ,$$
$$\phi_k(z)=\phi_w + A_1 e^{-\alpha_1 z} + A_2 e^{-\alpha_2 z} \ ,$$
$$\phi_i(z)=\phi_i + \sum_j^4 C_{i,j} e^{\gamma_{i,j} z}, \quad i<k \tag{41}$$
$$\phi_{k-1}=\phi_m, \quad \phi_{k-2}=\phi_o,\ldots,$$
$$\gamma_{k-1,j}=\beta_j, \quad \gamma_{k=2,j}=\alpha_j,\ldots$$

where α_i and β_i are the solutions of the characteristic polynomial (21) in the oil (water) phase and the microemulsion, respectively. There are $5k+2$ coefficients in (41), the $l_i, C_{i,j}$ and A_1, A_2. On the other hand, we have $5k$ conditions for the continuity of the profile and its derivatives, plus two boundary conditions. Nevertheless, it is *not* possible to find a solution for arbitrary k. If, for example, ω_s is chosen sufficiently large, $\phi(0)$ will obviously be in the interval $[-\phi_0,+\phi_0]$, so that only profiles with $k=1,3,5,\ldots$ can exist. For $k=1$, the profile is simply a wall-oil profile, for $k=3$ the wall is covered by an oil layer with approximately the same thickness as in the lamellar phase, etc. Solutions with $k \geq 3$ only exist in the vicinity of the phase transition of oil-water coexistence to the lamellar phase. A solution with $k=9$ is shown in Fig. 12.

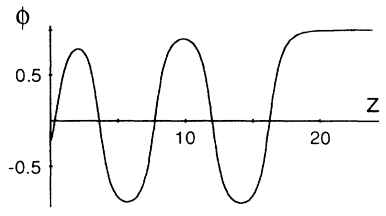

FIG. 12. Order-parameter profile in the vicinity of a wall, when the system is close to coexistence of oil-water and the lamellar phase, with $g_s=1.5$, $\omega_s=6.0$, and $\mu_s=0$. The calculations are for the piecewise parabolic model (5) with the parameters $c=1$, $g_m=-4.5$, $g_o=g_w=4.4$, $\omega_w=\omega_o=4$, $\omega_m=1$, $\phi_w=1$, $\phi_o=-1$, $f_0=0.7023$, and $\mu=0$.

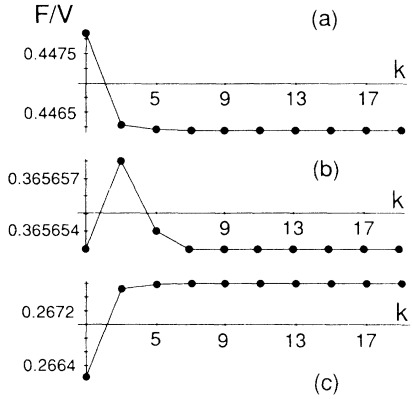

FIG. 13. Free energy (per unit surface area) of an order-parameter profile with k matching points (see text) between the wall and the bulk phase (oil). (a) Wall-oil interface is wet, $g_s=1.72$; (b) first-order wetting transition, $g_s=1.562\,54$; (c) wall-oil interface in nonwet, $g_s=1.41$. The parameters are the same as in Fig. 12, and $\mu_s=0$, $\omega_s=4$.

Consider first the case $\mu_s=0$. The free energy as a function of the number of oil layers is shown in Fig. 13 for various values of g_s, with $\omega_s>0$ fixed, at three-phase coexistence. The figure shows that $g_s>0$ favors wetting of the oil-wall interface by the lamellar phase. Within the numerical accuracy, all solutions with $k=7,9,\ldots$ have the same free energy, so that it is very difficult to decide whether the wetting transition is first or second order. However, Fig. 13(b) shows that there is a jump from $k=1$ to $k \geq 5$, which strongly suggests a first-order transition. Interpreted dynamically, the extremely weak dependence of the free energy on the number of layers for large k implies that while the first few layers will form very rapidly, the growth of further layers will be a very slow process. Such behavior has indeed been observed in the binary lipid-water system at the fluid-air interface [49,50].

The full surface phase diagram is shown in Fig. 14 for $\mu_s=0$. It demonstrates again that the lamellar phase wets only for $g_s>0$. For $\mu_s>0$, the oil phase is favored at the wall, which makes wetting by the lamellar phase

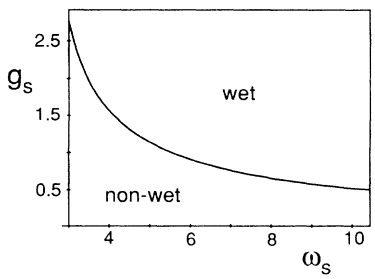

FIG. 14. Surface phase diagram at three-phase coexistence of oil, water, and lamellar phases, with $\mu_s=0$. The parameters are the same as in Fig. 12. The labels "wet" and "nonwet" refer to the wetting behavior of the wall-oil interface by the lamellar phase.

more difficult. For $\mu_s < 0$, wetting of the wall-oil interface by the water phase competes with wetting by the lamellar phase. This competition has not been studied yet.

VII. SUMMARY AND DISCUSSION

A simple Ginzburg-Landau model for oil-water-surfactant mixtures has been studied. This model uses a single, scalar order parameter, which is identified with the local difference of oil and water concentrations. The same model has been used previously to relate the wetting behavior of the oil-water interface by the microemulsion with the behavior of the bulk scattering intensity [13]. The predictions obtained from this study have by now been confirmed experimentally [51]. We have shown in this paper that the same Landau model can describe ordered phases in oil-water-surfactant mixtures, as there are a lamellar phase, a hexagonal phase of cylindrical micelles, a cubic phase (fcc) of spherical micelles, and bicontinuous cubic phases. Thus, all the principal phases observed in experiments on self-assembling systems are present in our model. Furthermore, we have made contact with the interfacial models of oil-water-surfactant mixtures, where all properties of the system are subsumed in the elastic properties of the surfactant monolayers. From a calculation of the free energy of curved oil-water interfaces, the elastic constants in the Helfrich Hamiltonian have all been determined. Finally, we have shown that the wetting behavior of the wall-oil interface by the lamellar phase can also be described by our model. Similar behavior has already been observed in two-component, water-surfactant systems [49,50].

Thus we believe that our Ginzburg-Landau model provides a "unified" theory of oil-water-surfactant mixtures. Many properties of these systems can also be described by other theories, like the lattice and interfacial models; however, they seem to be more limited in their range of applicability.

Recently, there have been several attempts [52–54] to derive expressions for the saddle-splay modulus $\bar{\kappa}$ and the bending rigidity κ of a liquid-vapor interface of *simple* fluids, in terms of the *microscopic interaction potential.* Far away from the critical point, the ratio $\bar{\kappa}/\kappa$ is found to be $-\frac{2}{3}$ in Refs. [52,53] and $+\frac{2}{3}$ in Ref. [54] (where the discrepancy in the sign will certainly be clarified in the future). The reason for this ratio to take a universal value is due to the sharp-kink approximation for the interfacial density profile used in the derivation. From our analysis of equilibrium droplets, it is clear that the equilibrium profile, or even the distortions of the profile, has to be taken into account to get reliable results for the interfacial free energy, and thus for the bending moduli.

ACKNOWLEDGMENTS

This work was supported in part by the Deutsche Forschungsgemeinschaft through Sonderforschungsbereich 266. We acknowledge many helpful discussions with Martin Kraus.

APPENDIX A: EQUIMOLAR RADIUS

The position R_e of the Gibbs dividing surface for a drop in d dimensions, embedded in a system of radius L, is defined by

$$\int_0^{R_e} dr\, r^{d-1}(\phi_+ - \phi) = \int_{R_e}^{L} dr\, r^{d-1}(\phi - \phi_-)\ , \tag{A1}$$

where ϕ_- and ϕ_+ denote the interior and the exterior bulk phases, respectively, i.e., the two solutions which minimize the grand potential $\Omega/V = f(\phi) - \mu\phi$. This implies

$$\begin{aligned} d\int_0^L dr\, r^{d-1}\phi &= \phi_- L^d + (\phi_+ - \phi_-)R_e^d\ , \\ R_e^d &= \frac{\int_0^L dr\, r^d \phi'}{\int_0^L dr\, \phi'}\ . \end{aligned} \tag{A2}$$

For $d = 1$ we use the notation z_e for R_e.

APPENDIX B: FINITE CURVATURE CORRECTIONS

We want to present here the details of the calculation of the correction to the free energy, which arise from the fact that for a drop or cylinder of finite radius the order-parameter profile deviates from the planar profile. The calculations are performed simultaneously for both spherical ($d = 3$) and cylindrical ($d = 2$) solutions of the Euler-Lagrange equations. As discussed in Sec. III, we assume that the order-parameter profile as well as the chemical-potential difference between inside and outside can be expanded in a power series in the inverse radius R^{-1} of droplets and cylinders around the planar profile (with $R^{-1} = 0$),

$$\begin{aligned} \phi &= \bar{\phi} + \delta\phi \\ &= \bar{\phi} + \frac{\phi_1}{R} + \frac{\phi_2}{R^2} + \cdots\ , \\ \mu &= \frac{\mu_1}{R} + \frac{\mu_2}{R^2} + \cdots \end{aligned} \tag{B1}$$

and that $f(\phi)$ and $g(\phi)$ can be expanded functionally:

$$f(\phi) = f(\bar{\phi}) + f'(\bar{\phi})\delta\phi + \tfrac{1}{2}f''(\bar{\phi})(\delta\phi)^2 + \cdots\ . \tag{B2}$$

These expansions are inserted into the Euler-Lagrange equation (6). Collecting terms of order R^{-n}, we obtain after shifting the origin to R, that is, $r \to r + R$, the following operators:

$$\begin{aligned} \Delta\phi &= \phi'' + (d-1)\frac{\phi'}{r+R} \\ &= \phi'' + (d-1)\frac{\phi'}{R} + O(R^{-2})\ , \\ \Delta^2\phi &= \phi'''' + 2(d-1)\frac{\phi'''}{r+R} \\ &\quad + \frac{(d-1)(d-3)}{(r+R)^2}\left[\phi'' - \frac{\phi'}{r+R}\right] \\ &= \phi'''' + 2(d-1)\frac{\phi'''}{R} + O(R^{-2})\ . \end{aligned} \tag{B3}$$

Contributions of order R^0 in the EL equation (6) vanish identically, because $\bar{\phi}$ satisfies the planar EL equation

$$2\bar{\phi}''''-2g(\bar{\phi})\bar{\phi}''-g'(\bar{\phi})(\bar{\phi}')^2+f'(\bar{\phi})=0 . \tag{B4}$$

To order R^{-1}, one has

$$\mu_1=2\phi_1''''+4(d-1)\bar{\phi}'''-2g(\bar{\phi})\phi_1''-2(d-1)g(\bar{\phi})\bar{\phi}' -2g'(\bar{\phi})(\phi_1\bar{\phi}''+\bar{\phi}'\phi_1')-g''(\bar{\phi})\phi_1(\bar{\phi}')^2+f''(\bar{\phi})\phi_1 . \tag{B5}$$

This result can be multiplied by $\bar{\phi}'$ and integrated over, so that after repeated integration by parts

$$\int dr\,\mu_1\bar{\phi}'=\int dr[-2\phi_1'\bar{\phi}''''-4(d-1)(\bar{\phi}'')^2 +2g(\bar{\phi})\phi_1'\bar{\phi}''-2(d-1)g(\bar{\phi})(\bar{\phi}')^2 +g'(\bar{\phi})\phi_1'\bar{\phi}'^2-f'(\bar{\phi}')\phi_1'] . \tag{B6}$$

A comparison with (B4) and (16a) yields

$$\int dr\,\mu_1\bar{\phi}'=-(d-1)\sigma_\infty . \tag{B7}$$

We can use the thermodynamic relation $p=\mu\phi_-$ for the interior bulk phase ϕ_-, together with (B1), to see that (B7) is equivalent with $\Delta p/R=-(d-1)\sigma_\infty+O(R^{-1})$, the Laplace equation (7) for a stable drop.

Next, we want to calculate the free energy of these solutions. We have to separate the free energy into a bulk and an interface contribution, F_b and F_s, respectively, where

$$F_b[\phi]=\frac{R^d}{d}[-\mu\phi_++f(\phi_+)] +\frac{L^d-R^d}{d}[-\mu\phi_-+f(\phi_-)] . \tag{B8}$$

ϕ_- and ϕ_+ are the values of the interior and the exterior bulk phases, which have been introduced in Appendix A. Here and in the following, we absorb a factor $2(d-1)\pi$ in all expressions of the free energy. Now, $\phi_\pm$ can be expanded in powers of R^{-1} just as the chemical potential μ in (B1),

$$\phi_\pm=\phi_{\pm,0}+\frac{\phi_{\pm,1}}{R}+\frac{\phi_{\pm,2}}{R^2}+\cdots . \tag{B9}$$

Since $\phi_{\pm,0}$ is a minimum of $f(\phi)$ and $f(\phi_{\pm,0})=0$, the expansion around this point is

$$f(\phi_\pm)=\tfrac{1}{2}f''(\phi_{\pm,0})\left[\frac{\phi_{\pm,1}}{R}+\frac{\phi_{\pm,2}}{R^2}\right]^2+\cdots . \tag{B10}$$

Furthermore, for an arbitrary function $h(r)$,

$$\int_{-R}^{L-R}dr(r+R)^{d-1}h(r) =\frac{R^d}{d}h(-R)+\frac{L^d-R^d}{d}h(L-R) -\int_{-R}^{L-R}dr\left[\frac{(r+R)^d-R^d}{d}\right]h'(r) , \tag{B11}$$

so that the bulk contribution to the free energy reads

$$\int dr(r+R)^{d-1}[-\mu\phi+\tfrac{1}{2}f''(\bar{\phi})(\delta\phi)^2] =F_b[\phi]+B_1+B_2 , \tag{B12}$$

where

$$B_1=\int dr\left[\frac{(r+R)^d-R^d}{d}\right]\mu\phi' ,$$
$$B_2=-R^{d-3}\int dr\,r\frac{d}{dr}[\tfrac{1}{2}f''(\bar{\phi})\phi_1^2]+O(R^{d-4}) . \tag{B13}$$

Here, we have already expanded B_2 in powers of R^{-1}; expanding B_1 also, we obtain

$$B_1=\mu_1\left[R^{d-2}\chi_1(0)+R^{d-3}\left[\frac{d-1}{2}\chi_2(0)+\chi_1(1)\right]\right] +\mu_2R^{d-3}\chi_1(0)+O(R^{d-4}) , \tag{B14}$$

where the notation

$$\chi_i(j)\equiv\int dr\,r^i\phi_j' \tag{B15}$$

has been used. The separation of bulk and interface terms is found to give the simplest expressions when the equimolar radius (see Appendix A) is used to define the interface position. Therefore, we identify R with R_e, and then drop the index again for convenience. For $R\to\infty$, R_e approaches z_e, the position of the equimolar surface of the planar interface,

$$z_e=\chi_1(0)/\chi_0(0) , \tag{B16}$$

compare (A2). With Eq. (A2), $R\equiv R_e$, and the substitution $r\to r+R$ one arrives at

$$R^d=\frac{\int(r+R)^d\phi'dr}{\int\phi'dr} ,$$
$$\int r\phi'dr=-\frac{d-1}{2R}\int r^2\phi'dr+O(R^{-2}) , \tag{B17}$$

or

$$\chi_1(0)=-\frac{1}{R}\left[\frac{d-1}{2}\chi_2(0)+\chi_1(1)\right]+O(R^{-2}) . \tag{B18}$$

This yields the simple result

$$B_1=O(R^{d-4}) . \tag{B19}$$

Now, the total free energy is given by

$$F[\phi]=\int_{-R}^{L-R}dr(r+R)^{d-1}\left[\left[\phi''+\frac{d-1}{r+R}\phi'\right]^2 +g(\phi)(\phi')^2+f(\phi)-\mu\phi\right] ; \tag{B20}$$

expanded to order R^{d-3}, this gives

$$F[\phi]=F_b[\phi]+F_s[\bar{\phi}]+\sum_{i=1}^{5}F_i ,$$

$$F_1=R^{d-2}\int dr[f'(\bar{\phi})\phi_1+2g(\bar{\phi})\bar{\phi}'\phi_1' +g'(\bar{\phi})\bar{\phi}'^2\phi_1+2\bar{\phi}''\phi_1'] , \tag{B21a}$$

$$F_2=(d-1)R^{d-3}\int dr\, r[f'(\bar{\phi})\phi_1+2g(\bar{\phi})\bar{\phi}'\phi_1'+g'(\bar{\phi})\bar{\phi}'^2\phi_1 +2\bar{\phi}''\phi_1'] , \tag{B21b}$$

$$F_3=R^{d-3}\int dr[f'(\bar{\phi})\phi_2+2g(\bar{\phi})\bar{\phi}'\phi_2'+g'(\bar{\phi})\bar{\phi}'^2\phi_2 +2\bar{\phi}''\phi_2''] , \tag{B21c}$$

$$F_4=R^{d-3}\int dr\left[-r\frac{d}{dr}[\tfrac{1}{2}f''(\bar{\phi})\phi_1^2]+\tfrac{1}{2}g''(\bar{\phi})\bar{\phi}'^2\phi_1^2 +g(\bar{\phi})\phi_1'^2+2g'(\bar{\phi})\bar{\phi}'\phi_1\phi_1'+\phi_1''^2\right] , \tag{B21d}$$

$$F_5=2(d-1)R^{d-3}\int dr[\bar{\phi}'\phi_1''+\bar{\phi}''\phi_1'] , \tag{B21e}$$

where all terms which contain only $\bar{\phi}$ are collected in $F_s[\bar{\phi}]$; they have already been calculated in Sec. III. To simplify this lengthy expression, we first use (B4). This equation, multiplied by ϕ_i $(i=1,2)$ and integrated over, yields

$$\int dr[f'(\bar{\phi})\phi_i+2g(\bar{\phi})\bar{\phi}'\phi_i'+g'(\bar{\phi})\bar{\phi}'^2\phi_i+2\bar{\phi}''\phi_i'']=0 \tag{B22}$$

so that F_1 and F_3 vanish identically. Similarly, again with (B4)

$$\int dr\, r[f'(\bar{\phi})\phi_1+2g(\bar{\phi})\bar{\phi}'\phi_1'+g'(\bar{\phi})\bar{\phi}'^2\phi_1+2\bar{\phi}''\phi_1''] =-\int dr\, 2[g(\bar{\phi})\bar{\phi}'\phi_1+2\bar{\phi}''\phi_1'] \tag{B23}$$

which simplifies F_2:

$$F_2=-2(d-1)R^{d-3}\int dr[g(\bar{\phi})\bar{\phi}'\phi_1+2\bar{\phi}''\phi_1'] . \tag{B24}$$

F_5 also vanishes identically. The only term left over is F_4. Multiplication of (B5) with ϕ_1 and integration by parts gives

$$2(d-1)\int dr[g(\bar{\phi})\bar{\phi}'\phi_1+2\bar{\phi}''\phi_1']=I_1+I_2 , \tag{B25}$$

where

$$I_1=\int dr[f''(\bar{\phi})\phi_1^2-\mu_1\phi_1] , \tag{B26}$$

$$I_2=\int dr[g''(\bar{\phi})\bar{\phi}'^2\phi_1^2+4g'(\bar{\phi})\bar{\phi}'\phi_1\phi_1' +2g(\bar{\phi})\phi_1'^2+2\phi_1''^2] . \tag{B27}$$

Finally, (B5) implies

$$f''(\phi_{\pm,0})\phi_{\pm,1}-\mu_1=0 , \tag{B28}$$

and (B26), integrated by parts, gives

$$I_1=\int dr\, r\left[-\frac{d}{dr}(f''(\bar{\phi})\phi_1^2)+\mu_1\phi_1'\right] \tag{B29}$$

so that

$$F[\phi]=F_b[\phi]+F_s[\bar{\phi}] -AR^{-2}\int dr\{(d-1)[g(\bar{\phi})\bar{\phi}'\phi_1+2c\bar{\phi}''\phi_1'] +\tfrac{1}{2}\mu_1 r\phi_1'\} \tag{B30}$$

where A is the area of the interface. This is the result quoted in Sec. III.

APPENDIX C: AN EXACT SOLUTION FOR $c=0$

For the square-gradient theories [i.e., $c=0$, $g(\phi)=g_0>0$] with a double-well potential, the expressions (16) for $\bar{\kappa}$ and λ have been known for quite a while [32,33]. However, we present here the corrections which are due to the distortion of the profile for finite radii for the first time. In the double-parabola approximation, we have (with $g_0=1$)

$$F[\phi]=\int_V d^dr[(\nabla\phi)^2+f(\phi)-\mu\phi] ,$$
$$f(\phi)=\begin{cases}\omega_+(\phi-\phi_+)^2, & \phi>0\\ \omega_-(\phi-\phi_-)^2, & \phi<0 ,\end{cases} \tag{C1}$$

where

$$\omega_+\phi_+^2=\omega_-\phi_-^2 \tag{C2}$$

so that the free energy density f is continuous at $\phi=0$. In this case, not only the planar profile but also the profiles of both cylinder and sphere can be calculated analytically. This gives us the possibility to compare our results (16a), (16d), and (18) with exact free energies.

$f(\phi)-\mu\phi$ can be written as

$$f(\phi)-\mu\phi=\begin{cases}\omega_+(\phi-\phi_{+,\mu})^2+f_+, & \phi>0\\ \omega_-(\phi-\phi_{-,\mu})^2+f_-, & \phi<0,\end{cases}$$
$$\phi_{\pm,\mu}=\phi_\pm+\frac{\mu}{2\omega_\pm} , \tag{C3}$$
$$f_\pm=-\mu\phi_\pm-\frac{\mu^2}{4\omega_\pm} .$$

The order-parameter profiles are given by two functions, $\phi_>(r)>0$, and $\phi_<(r)<0$, which are patched together at $\phi=0$ such that both the profile and its first derivative are continuous. Both functions satisfy the EL equation $2\Delta\phi=[f'(\phi)-\mu]$ for the respective parabola.

The solution for the planar profile reads $(\mu=0)$

$$\phi=\begin{cases}\phi_-(1-e^{\alpha_+x}), & x<0\\ \phi_+(1-e^{-\alpha_-x}), & x>0 ,\end{cases}$$
$$\alpha_\pm=\sqrt{\omega_\pm} \tag{C4}$$

while the free energy per unit area (the surface tension) is given by

$$\sigma=\sqrt{\omega_+}\phi_+^2+\sqrt{\omega_-}\phi_-^2 . \tag{C5}$$

Finally, one has

$$\int_{-\infty}^{\infty} dz\, z^n \phi'^2 = \omega_+ \phi_+^2 \frac{n!}{(2\alpha_+)^{n+1}} + (-1)^n \omega_- \phi_-^2 \frac{n!}{(2\alpha_-)^{n+1}} \tag{C6}$$

so that the elastic moduli are found to be

$$\lambda = \phi_+^2 - \phi_-^2 ,$$
$$\bar{\kappa} = \frac{\phi_+^2}{2\sqrt{\omega_+}} + \frac{\phi_-^2}{2\sqrt{\omega_-}} \tag{C7}$$

while the bending rigidity κ vanishes identically.

The solution for the spherical drop is given by

$$\phi(r) = \begin{cases} \phi_{-,\mu} \left[1 - \dfrac{R}{\sinh(\alpha_- R)} \dfrac{\sinh(\alpha_- r)}{r} \right], & r \in [0, R] \\ \phi_{+,\mu} \left[1 - \dfrac{R}{e^{-\alpha_+ R}} \dfrac{e^{-\alpha_+ r}}{r} \right], & r \in [R, \infty] . \end{cases} \tag{C8}$$

Continuity of the first derivative at $\phi = 0$ implies

$$\phi_{+,\mu}(\alpha_+ + R^{-1}) = -\phi_{-,\mu}[\alpha_- \coth(\alpha_- R) - R^{-1}]$$
$$= -\phi_{-,\mu}(\alpha_- - R^{-1}) + O(e^{-2\alpha_- R}) . \tag{C9}$$

Since R is large compared to the correlation length α_-^{-1}, terms of order $O(e^{-\alpha_- R})$ can be neglected. Therefore, we find for the chemical potential with (C3) that

$$\mu = \frac{2(\phi_- - \phi_+)\omega_+ \omega_-}{R\sqrt{\omega_+ \omega_-}(\sqrt{\omega_+} + \sqrt{\omega_-}) - \omega_+ + \omega_-} + O(e^{-2\alpha_- R}) . \tag{C10}$$

Then, the expansion $\mu = \mu_1 / R + \cdots$ yields

$$\mu_1 = \frac{2(\phi_- - \phi_+)\sqrt{\omega_+ \omega_-}}{\sqrt{\omega_+} + \sqrt{\omega_-}} . \tag{C11}$$

The calculation of the free energy from Eq. (11) implies for the interfacial free energy

$$\frac{F_s}{4\pi} = R^2[-\phi_{-,\mu}\phi'_<(R)] + R^2[\phi_{+,\mu}\phi'_>(R)]$$
$$= R^2(\sqrt{\omega_+}\phi_{+,\mu}^2 + \sqrt{\omega_-}\phi_{-,\mu}^2) + R(\phi_{+,\mu}^2 - \phi_{-,\mu}^2) , \tag{C12}$$

where the terms of order $O(e^{-\alpha_- R})$ have been dropped. Since

$$\omega_\pm \phi_\pm^2 = f_\pm + \omega_\pm \phi_{\pm,\mu}^2 \tag{C13}$$

we finally arrive at

$$\frac{F_s}{4\pi} = R^2\sigma + R\lambda - R^2\left[\frac{f_+}{\sqrt{\omega_+}} + \frac{f_-}{\sqrt{\omega_-}}\right] + R\left[\frac{f_-}{\omega_-} - \frac{f_+}{\omega_+}\right] . \tag{C14}$$

We now want to compare with the result (18) obtained by expanding around the planar profile. This will give us an idea of how important the correction terms are. We expand (C8) around the planar profile (C4) to order R^{-1}, which gives

$$\phi(r+R) = \bar{\phi}(r) + \frac{\phi_1(r)}{R} + O(R^{-2}) + O(e^{-\alpha_- R})$$
$$\phi_1(r) = \begin{cases} \dfrac{\mu_1}{2\omega_-}(1 - e^{\alpha_- r}) + \phi_- r e^{\alpha_- r}, & r < 0 \\ \dfrac{\mu_1}{2\omega_+}(1 - e^{-\alpha_+ r}) + \phi_+ r e^{-\alpha_+ r}, & r > 0 . \end{cases} \tag{C15}$$

The correction terms in (18) can then be calculated:

$$-2\int \bar{\phi}'\phi_1 dr = -\bar{\kappa} - \frac{\mu_1}{2}\left[\frac{\phi_+}{\omega_+} - \frac{\phi_-}{\omega_-}\right] ,$$
$$-\frac{\mu_1}{2}\int r\phi_1' dr = \frac{\mu_1}{2}\left[\frac{\phi_+}{\omega_+} - \frac{\phi_-}{\omega_-}\right] - \frac{\mu_1^2}{4}\left[\frac{1}{(\omega_+^3)^{1/2}} + \frac{1}{(\omega_-^3)^{1/2}}\right] . \tag{C16}$$

The simplest case is a system with oil-water symmetry, i.e., with a symmetric free-energy density f, so that $\omega_+ = \omega_-$ and $\phi_- = -\phi_+$. In this case we have

$$\mu_1 = -2\phi_+\sqrt{\omega_+} ,$$
$$\bar{\kappa} = \frac{\phi_+^2}{\sqrt{\omega_+}} . \tag{C17}$$

Equation (C14) yields in this case

$$\frac{F_s}{4\pi} = R^2\sigma - 2\frac{\phi_+^2}{\sqrt{\omega_+}} \tag{C18}$$

while the correction terms are

$$-2\int \bar{\phi}'\phi_1 dr = -\bar{\kappa} + 2\frac{\phi_+^2}{\sqrt{\omega_+}} ,$$
$$-\frac{\mu_1}{2}\int r\phi_1' dr = -4\frac{\phi_+^2}{\sqrt{\omega_+}} . \tag{C19}$$

We find that the two results are in complete agreement. The magnitude of the corrections due to the deformation of the profile is by a factor of 3 *larger* than $\bar{\kappa}$ itself.

[1] *Physics of Amphiphilic Layers,* edited by J. Meunier, D. Langevin, and N. Boccara, Springer Proceedings in Physics Vol. 21 (Springer, Berlin, 1987).

[2] *Modern Ideas and Problems in Amphiphilic Science,* edited by W. M. Gelbart, D. Roux, and A. Ben-Shaul (Springer, Berlin, in press).

[3] D. M. Anderson, H. T. Davis, L. E. Scriven, and J. C. C. Nitsche, Adv. Chem. Phys. 77, 337 (1990), and references

therein.
[4] *Statistical Mechanics of Membranes and Surfaces,* edited by D. R. Nelson, T. Piran, and S. Weinberg (World Scientific, Singapore, 1989).
[5] R. Lipowsky, Nature **349**, 475 (1991).
[6] B. Alberts, D. Bray, J. Lewis, R. Raff, K. Roberts, and J. D. Watson, *Molecular Biology of the Cell* (Garland, New York, 1983).
[7] A. M. Polyakov, *Gauge Fields and Strings* (Harwood, New York, 1988).
[8] B. Widom, J. Chem. Phys. **84**, 6943 (1986); K. A. Dawson, B. L. Walker, and A. Berera, Physica A **165**, 320 (1990).
[9] K. Chen, C. Ebner, C. Jayaprakash, and R. Pandit, J. Phys. C **20**, L361 (1987); Phys. Rev. A **38**, 6240 (1988).
[10] A. Ciach, J. S. Høye, and G. Stell, J. Phys. A **21**, L777 (1988); J. Chem. Phys. **90**, 1214 (1989).
[11] G. Gompper and M. Schick, Phys. Rev. Lett. **62**, 1647 (1989); Phys. Rev. B **41**, 9148 (1990); Phys. Rev. A **42**, 2137 (1990).
[12] M. W. Matsen and D. E. Sullivan, Phys. Rev. A **41**, 2021 (1990); M. Laradji, H. Guo, M. Grant, and M. Zuckermann, *ibid.* **44**, 8184 (1991).
[13] G. Gompper and M. Schick, Phys. Rev. Lett. **65**, 1116 (1990).
[14] W. Helfrich, Z. Naturforsch. C **28**, 693 (1973).
[15] S. A. Safran, L. A. Turkevich, and P. A. Pincus, J. Phys. (Paris) Lett. **45**, L69 (1984); S. A. Safran, Phys. Rev. A **43**, 2903 (1991).
[16] S. A. Safran, D. Roux, M. E. Cates, and D. Andelman, Phys. Rev. Lett. **57**, 491 (1986); D. Andelman, M. E. Cates, D. Roux, and S. A. Safran, J. Chem. Phys. **87**, 7229 (1987); S. T. Milner, S. A. Safran, D. Andelman, M. E. Cates, and D. Roux, J. Phys. (Paris) **49**, 1065 (1988); P. Chandra and S. A. Safran, Europhys. Lett. **17**, 691 (1992).
[17] D. Huse and S. Leibler, J. Phys. (Paris) **49**, 605 (1988).
[18] L. Golubović and T. C. Lubensky, Phys. Rev. B **39**, 12 110 (1989); Europhys. Lett. **10**, 513 (1989); Phys. Rev. A **41**, 4343 (1990).
[19] Z. G. Wang and S. Safran, Europhys. Lett. **11**, 425 (1990).
[20] Our expression (1) agrees with the usual form of the Helfrich Hamiltonian for *tensionless* monolayers $\mathcal{H}=\int dS\,[2\kappa(H-H_0)^2+\bar{\kappa}K]$ with $H_0=1/R_0$, in the special case $\sigma=2\kappa R_0^{-2}$.
[21] F. David and S. Leibler, J. Phys. II (Paris) **1**, 959 (1991).
[22] G. Gompper and S. Zschocke, Europhys. Lett. **16**, 731 (1991).
[23] K. Kawasaki and T. Kawakatsu, Physica A **164**, 549 (1990).
[24] I. Szleifer, D. Kramer, A. Ben-Shaul, D. Roux, and W. M. Gelbart, Phys. Rev. Lett. **60**, 1966 (1988).
[25] The effect of electrostatic interactions on the curvature elasticity has been studied by H. N. W. Lekkerkerker, Physica A **159**, 319 (1989); **167**, 384 (1990); D. Bensimon, F. David, S. Leibler, and A. Pumir, J. Phys. (Paris) **51**, 689 (1990); P. Pincus, J.-F. Joanny, and D. Andelman, Europhys. Lett. **11**, 763 (1990); B. Duplantier, R. E. Goldstein, V. Romero-Rochín, and A. I. Pesci, Phys. Rev. Lett. **65**, 508 (1990).
[26] Estimates of the bending moduli in polymer systems have been discussed by S. T. Milner and T. A. Witten, J. Phys. (Paris) **49**, 1951 (1988); Z. G. Wang and S. A. Safran, *ibid.* **51**, 185 (1990); J. Chem. Phys. **94**, 679 (1991).
[27] K. Chen, C. Jayaprakash, R. Pandit, and W. Wenzel, Phys. Rev. Lett. **65**, 2736 (1990).
[28] A model with three order parameters has been suggested in Refs. [23,29].
[29] T. Kawakatsu and K. Kawasaki, Physica A **167**, 690 (1990).
[30] In the vicinity of the tricritical point, the results of a Landau theory with $g=\text{const}>0$ and $c=0$ agree very well with the experimental data, see H. Kleinert, J. Chem. Phys. **84**, 964 (1986).
[31] The vicinity of Lifshitz critical end points and Lifshitz tricritical points has been studied within the Landau model (2) by G. Gompper, R. Holyst, and M. Schick, Phys. Rev. A **43**, 3157 (1991).
[32] M. Teubner and R. Strey, J. Chem. Phys. **87**, 3195 (1987).
[33] The parabolic approximation has been introduced in the context of wetting by R. Lipowsky, Z. Phys. B **55**, 345 (1984).
[34] When $\sigma[R]$ is identified with the interfacial tension for the planar interface, the Laplace equation is exact only for a particular choice of the dividing surface, the "surface of tension," see Ref. [35].
[35] J. S. Rowlinson and B. Widom, *Molecular Theory of Capillarity* (Clarendon, Oxford, 1982).
[36] M. P. A. Fisher and M. Wortis, Phys. Rev. B **29**, 6252 (1984).
[37] H.-W. Diehl, D. M. Kroll, and H. Wagner, Z. Phys. B **36**, 329 (1980).
[38] S. C. Lin and M. J. Lowe, J. Phys. A **16**, 347 (1983).
[39] R. K. P. Zia, Nucl. Phys. B **251**, 676 (1985).
[40] W. Helfrich, in *Physics of Defects,* edited by R. Balian, M. Kléman, and J.-P. Poirier (North-Holland, Amsterdam, 1981).
[41] The calculation of effective interactions between interfaces has been studied extensively in the context of wetting transitions, see Refs. [42–44].
[42] E. Brezin, B. I. Halperin, and S. Leibler, J. Phys. (Paris) **44**, 775 (1983).
[43] R. Lipowsky, D. M. Kroll, and R. K. P. Zia, Phys. Rev. B **27**, 4499 (1983).
[44] M. E. Fisher and A. Jin, Phys. Rev. B **44**, 1430 (1991).
[45] M. E. Fisher and B. Widom, J. Chem. Phys. **50**, 3756 (1969); J. Stephenson, J. Math. Phys. **11**, 420 (1970).
[46] It has been shown in Ref. [31] that for a particular choice of parameters in (4) this profile is an exact solution of the EL equations.
[47] S. Dietrich, in *Phase Transitions and Critical Phenomena,* edited by C. Domb and J. L. Lebowitz (Academic, London, 1988), Vol. 12.
[48] G. Forgacs, R. Lipowsky, and Th. M. Nieuwenhuizen, in *Phase Transitions and Critical Phenomena,* edited by C. Domb and J. L. Lebowitz (Academic, London, 1991), Vol. 14.
[49] P. S. Pershan, Coll. Phys. **50**, C7-1 (1989).
[50] G. Cevc, W. Fenzl, and L. Sigl, Science **249**, 1161 (1990).
[51] K.-V. Schubert and R. Strey, J. Chem. Phys. **95**, 8532 (1991).
[52] J. B. Keller and G. J. Merchant, J. Stat. Phys. **63**, 1039 (1991).
[53] M. Napiórkowski and S. Dietrich (unpublished).
[54] E. M. Blokhuis and D. Bedeaux, J. Chem. Phys. **95**, 6986 (1991).